Received: 15 January 2024 | Revised: 8 July 2024 | Accepted: 5 August 2024
DOI: 10.1111/ejss.13558

RESEARCH ARTICLE

European Journal of Soil Science | WILEY

How does soil water retention change over time? A three-year field study under several production systems

Clémence Pirlot | **Anne-Catherine Renard** | **Caroline De Clerck** | **Aurore Degré**

Uliège, Gembloux Agro-Bio Tech, TERRA Teaching and Research Centre, Gembloux, Belgium

Correspondence
Clémence Pirlot, Uliège, Gembloux Agro-Bio Tech, TERRA Teaching and Research Centre, 2, Passage des Déportés, 5030 Gembloux, Belgium.
Email: clemence.pirlot@uliege.be

Funding information
Société Publique de Gestion de l'Eau (SPGE)

Abstract

Agricultural practices and meteorological conditions affect soil structure and soil hydraulic properties. However, their temporal evolution is rarely studied, and even less in the field. Thus, their dynamics are rarely taken into account in models, often leading to inconsistent results and poor decision making. In this study, the temporal evolution of water retention properties and soil structure was monitored over a 3-year period under several contrasting production systems. Soil Water Retention Curves (SWRCs) obtained directly in the field (with soil water content and potential sensors) were compared with theoretical SWRCs predicted by pedotransfer functions (PTFs) and laboratory SWRCs measured on undisturbed samples. Bulk densities were measured every 2 months. Results indicate a high degree of variability in SWRCs over time and between production systems. The results suggest that variations in the soil water retention behaviour can be induced by crop differentiation, weed control, crop residue management, compaction during harvest, or the introduction of temporary grassland. Contrasting climatic conditions between 2021 (water excess), 2022 (severe drought) and 2023 (intermediate) provided a unique opportunity to study the resilience of the crop systems to extreme climatic conditions. Different soil drying dynamics were observed and some agricultural practices were identified as influencing the soil water retention behaviour for at least 2 years. Comparison of SWRCs showed that the theoretical curves obtained from PTFs are not a good representation of the field SWRCs, especially for less conventional agricultural practices. The laboratory curves are closer with similar trends. However, these SWRCs are not optimal for investigating the temporal evolution of water retention properties. This research also shows that agricultural practices and crops can be levers for contributing to greater food resilience against future climatic conditions. Therefore, to assess the relevance of production systems for tomorrow's needs, studies should focus on the impact of multi-cropping systems on water retention dynamics in the field.

KEYWORDS
agricultural practices, crop differentiation, field monitoring, food resilience, sensors, soil structure, soil water retention curve, water stress, weed management

1 | INTRODUCTION

1.1 | General challenge

In the last decade, alternative agricultural practices have become more common to provide more sustainable production systems with long and diverse crop rotations, cover crops, or limited chemical inputs (Piñeiro et al., 2020). In addition, climate change will put significant pressure on crop water availability due to high variability in rainfall and increased evaporation. To improve the water resilience of the system for the future, priority needs to be given to understand how these agricultural practices affect soil water behaviour (Chandrasekhar et al., 2018; Heitman et al., 2023).

Highlights

- How do agricultural practices and crops affect soil water retention properties over time?
- This study reports the outputs of 3 years of continuous field monitoring under contrasting production systems.
- Differences in water retention between crops, agricultural practices and over a season were determined.
- Agriculture has a great potential to contribute to food system resilience against climate change.

1.2 | Hydraulic properties

The hydraulic properties of soils are the basis for modelling water fluxes and solute transport in soils for decision-making. In particular, they influence evaporation, groundwater recharge, contaminant transport, and water availability for plants (Ciocca et al., 2014; Whalley et al., 2013). A Soil Water Retention Curve (SWRC) shows the relationship between water content and matric potential and provides a better understanding of water behaviour in the soil. It gives information on soil structure, water retention capacity, wilting point, and available water content (Rabot et al., 2018).

1.3 | Influencing factors

The SWRC is usually considered to be an invariable soil property, determined in the laboratory or predicted by pedotransfer functions (PTFs). However, several studies have shown the influence of agricultural practices, vegetation growth, and climatic conditions such as rainfall, freeze–thaw and wet-drying cycles (WDs) on soil hydraulic properties and structure (Alletto et al., 2015; Alskaf et al., 2021; Huang et al., 2021; Jensen et al., 2020; Pečan et al., 2023; Tifafi et al., 2017). The main factors influencing hydraulic properties found in the literature are:

1.3.1 | Tillage

Ploughing creates an abundance of large pores and unstable aggregates that collapse during rainfall. During post-tillage WDs, bulk density (ρ_b) and water retention capacity increase due to a reduction in effective soil porosity and hysteresis (Huang et al., 2021; Zhang et al., 2017). This creates a large number of interconnected pores, which improves water retention (Sandin et al., 2017; Zhang et al., 2018). After each WDs, the steepness of SWRCs increases, indicating a reduction in the rewetting rate (Herbrich & Gerke, 2017; Kool et al., 2019). However, no-till (NT) systems have a higher water retention capacity due to the accumulation of organic matter (OM) near the soil surface and a well-developed pore system (Gozubuyuk et al., 2015; Zhang et al., 2018). Retention capacity fluctuates less over time in NT due to the greater rigidity of the pore system (Huang et al., 2021). However, NT may increase the risk of compaction in the long term, resulting in finer soil porosity and greater water retention (Blanco-Canqui & Wortmann, 2020).

1.3.2 | Root system

Pečan et al. (2023) showed that the shape of the SWRCs depends more on the root system development and environmental conditions during the seasons than on the tillage systems. Different stages of root development have also been shown to affect the hydraulic properties of soils by clogging pores, breaking up aggregates, and forming macropores (Ajayi et al., 2019; Lu et al., 2020).

1.3.3 | Crop and rotation

Diverse crops rotations improve pore connectivity and increase OM and microbial activity, enhancing infiltration and water retention capacity (Ball et al., 2005; McDaniel et al., 2014). Crop succession affects the SWRC, and a rotation with 2 years of grassland was found to have a higher available water retention capacity than a mixed crop rotation (Herbrich & Gerke, 2017; Schwärzel et al., 2011). When grassland was converted to bare soil, the water retention capacity decreased, whereas inverse conversion showed no change despite an increase in bulk density (Jensen et al., 2020). Bacq-Labreuil et al. (2021) found an increase in porosity, pore size diversity, and pore connectivity when bare soil was converted to grassland. However, soil structure was not affected by the conversion to arable crops.

1.3.4 | Soil compaction

After compaction on bare or covered ground (caused by machines or animals), the physical properties of the soil undergo alterations that persist for more than 2 years (Keller et al., 2021). The extent of these alterations depends on the compaction force applied resulting in significant differences in the physical properties of the soil. Over time, the compaction effect decreases with natural recovery (Hu et al., 2018). However, these recovery processes can take decades or even centuries (Keller et al., 2021; Meurer, Barron, et al., 2020).

1.4 | The conventional approaches for investigating temporal variability

The temporal variability of hydraulic properties is generally studied in the laboratory, using small samples in undisturbed structures (Ajayi et al., 2019; Geris et al., 2021; Kool et al., 2019). The drying branch of the SWRC is obtained at different times, generally before and after the event under investigation. Then, these SWRCs are fitted with empirical models, the most widely used being the model of van Genuchten (Jensen et al., 2019; Pires et al., 2017; van Genuchten, 1980). However, the results obtained are often inconsistent between studies due to the spatial and temporal variability of soil properties or the type of measurements performed (Chandrasekhar et al., 2018; Strudley et al., 2008). Furthermore, a large variability in SWRC can be obtained between different laboratories due to non-harmonised and non-standardised procedures (Guillaume et al., 2023). Temporal variability can also be studied using SWRCs obtained by PTFs based on easily measurable soil properties (Tóth et al., 2015). These functions represent the SWRCs with high accuracy (93%), but only for those obtained under laboratory conditions (Ahmed et al., 2021; Dashtaki et al., 2010; Tian et al., 2021).

1.5 | Importance for modelling

The few studies that have included the dynamics of hydraulic properties in the models have shown better predictions and more reliable results (Alletto et al., 2015; Geris et al., 2021; Schwärzel et al., 2011; Schwen et al., 2011). The importance of developing models capable of simulating the temporal dynamics of soil hydraulic properties has been demonstrated (Hannes et al., 2016; Jarvis et al., 2022; Meurer, Chenu, et al., 2020). Recently, Vogel et al. (2023) presented a physically based concept to better describe these properties under non-equilibrium hydraulic conditions. However, the parameterisation of water flow and soil structure in models remains a challenge.

1.6 | Comparison of field measurements with other methods

Some studies have focused on the measurement of in-situ SWRCs and their comparison with curves obtained in the laboratory or from PTFs (Bordoni et al., 2017; Huang et al., 2021; Pečan et al., 2023). Significant differences were observed due to hysteresis, WDs, and changes in soil structure over time (Basile et al., 2003). Hysteresis describes the non-unique relationship between water content and matric potential during drying and wetting phases due to pore heterogeneity, a difference in contact angle, air entrained in the pore system, and the swelling shrinking properties of the soil (Basile et al., 2003; Dey et al., 2017; Hannes et al., 2016; Zhao et al., 2020). As a result, laboratory or theoretical SWRCs failed to represent the dynamics of water retention and were insufficient to explain how agricultural practices might affect water behaviour (Ahmed et al., 2021; Alletto et al., 2015; Hedayati et al., 2020; Huang et al., 2021; Iiyama, 2016; Pečan et al., 2023; Zhang et al., 2018).

1.7 | Gaps in the literature

In both cases (laboratory and field conditions), studies generally investigate the dynamic evolution of SWRCs for isolated agricultural practices, such as different types of tillage, compaction, or a change in land use (Huang et al., 2021; Jensen et al., 2020; Keller et al., 2021). Yet, it is essential to examine the impact of the whole production system on the evolution of hydrodynamic properties and soil structure in order to assess its resilience for the future. Furthermore, these investigations often focus on a short-term period, such as one or two growing seasons, and on the topsoil layers (Geris et al., 2021; Huang et al., 2021; Zhang et al., 2018). However, production systems can have impacts on longer time scales and at greater depths (Bordoni et al., 2017; Jirků et al., 2013; Wahren et al., 2009).

1.8 | Objectives

Therefore, this study aims (1) to evaluate the impact of several whole production systems and contrasting climatic conditions on the temporal evolution of SWRCs in the field over 3 years and (2) to compare the field curves with those obtained by PTFs prediction and under laboratory conditions on undisturbed samples.

TABLE 1 Physico-chemical properties of the three soil layers studied.

	L1	L2	L3
Depth	0–30	30–60	60–90
Texture	Fine silty clay		
Clay (%)	13.8	13.1	19.2
Silt (%)	78.3	80.4	74.5
Sand (%)	7.9	6.4	6.2
Organic carbon (g/kg)	12.3	5.24	3.35
CEC (meq/100 g)	9.4	8.3	10.6
pH water	7.6	7.8	7.9
Bulk density (g/cm^3)	1.38 ± 0.03	1.54 ± 0.01	1.64 ± 0.01
Porosity	0.47 ± 0.01	0.42 ± 0.01	0.38 ± 0.00

2 | MATERIALS AND METHODS

2.1 | Experimental setup

The experiment has been conducted on an agricultural silt soil located at the EcoFoodSystem experimental plots (50°56′50.6″ N, 4°70′93.2″ E) of the Terra teaching and research centre in Gembloux, Belgium. The soil is a Cutanic Luvisol according to the World Reference Base for Soil Resources (FAO, 2015). The climate is temperate oceanic with an average annual temperature of 10.2°C and an average annual rainfall of 837 mm. Meteorological data were collected at the Ernage-Gembloux station, located less than 2 km away from the experimental plots. The physico-chemical properties of the first three soil layers were determined at the beginning of the experiment in 2021 and are given in Table 1.

Three contrasting production systems have been implemented as part of the EcoFoodSystem experiment (Figure 1). They integrate several sustainable agricultural practices such as 8-year crop rotations, cover crops, and periods of sheep grazing. The rotations have been designed to meet the food needs of the future through multiple agricultural trajectories, based on a study carried out by EAT LANCET (Eat Lancet Commission, 2019). The first system is called 'reference'. The animal is integrated into this system through the flow of agricultural by-products and manure. Two variants are implemented for it, allowing (ref herb) or not (ref) the use of chemical herbicides only. Other types of pesticides are not allowed. The second system is called 'Integrated Crop Livestock System (ICLS)'. Here, the animal is integrated through grazing periods of cover crops and two-and-a-half years of temporary grassland. This rotation is managed without using any chemical pesticides. The third rotation, called 'vegan', is based on a future where animals are no longer part of the system. The rotation is designed to meet human nutritional needs. The 'vegan' designation is derived solely from the use of crops intended exclusively for human consumption and the absence of inputs of animal products such as manure. This rotation is also managed without using any chemical pesticides.

In September 2020, the four systems were implemented on eight adjacent 18 × 84 m plots. Two crops of each rotation were implemented each year, corresponding to two temporalities (rotation starting in year 1 [T1] and year 5 [T2] of the 8-year rotation). To homogenise the plots, 1 year of winter wheat was grown prior to the start of the experiment. Leaf area index and aerial biomass measurements showed a high degree of uniformity in winter wheat growth across the eight plots. In addition, winter wheat will be grown in all systems every 2 years, acting as an internal reference making comparisons between systems possible. This study covers the first 3 years of the crop rotation (2021–2022–2023).

Agricultural operations made on the eight plots during the experiment are illustrated in Figure 2.

2.2 | Soil measurements

The eight plots were instrumented to measure water content and matric potential continuously at depths of 30, 60, and 90 cm. At the beginning of September 2020, a 1.2 m deep trench was dug on each plot in the middle of the plot width and 30 m from the edge.

Teros 12 capacitance sensors (Meter Group, Inc., Pullman, WA, USA) were used to monitor soil volumetric water content (VWC). These sensors use a 70 MHz frequency and also measure soil temperature and electrical conductivity. They measure VWC over a range of 0.00–0.70 m^3/m^3 with a resolution of 0.001 m^3/m^3 and an accuracy of 0.01–0.02 m^3/m^3 with calibration. Calibration

European Journal of Soil Science — WILEY

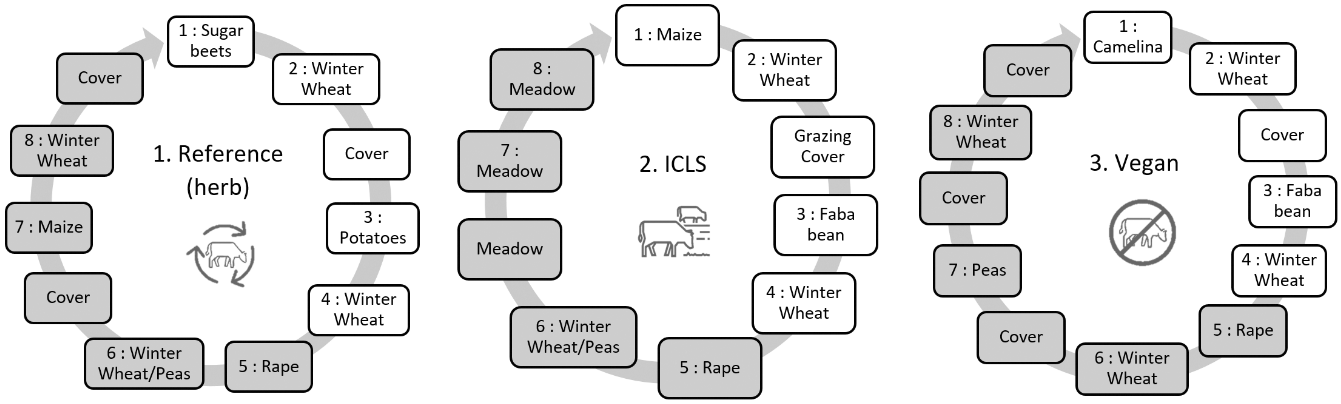

FIGURE 1 Eight-year rotations of the three contrasting production systems implemented as part of the EcoFoodSystem experiment. The clear boxes represent temporality 1 (T1) of each rotation (years 1–4). The grey shaded boxes represent temporality 2 (T2) of each rotation (years 5–8).

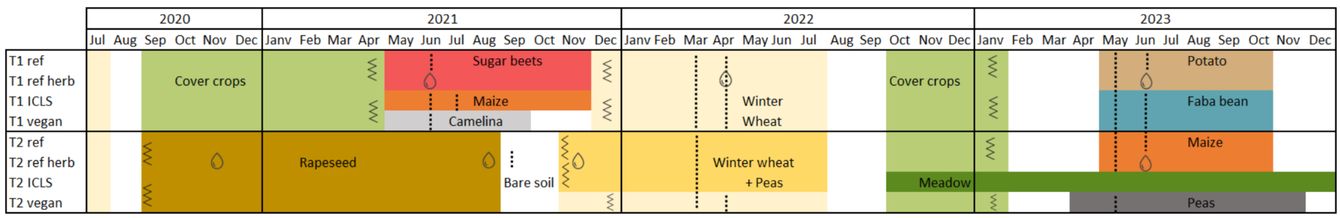

FIGURE 2 Agricultural practices and crops from July 2020 to December 2023 on the eight EcoFoodSystem experimental plots. The colours represent the different crops, the zigzags indicate ploughing to a depth of 25 cm, the dotted lines refer to soil treatment (hoeing, harrowing or rotary hoeing) to a maximum depth of 5 cm and the drops correspond to herbicide application.

was performed according to Meter Group instructions for soils at the three depths investigated. R^2 values between 0.998 and 0.999 were obtained.

Each probe has an influence volume of 1010 cm^3. Considering that the plots in the experiment are 18 × 84 m and have a horizon of 0.3 m, the volume of soil in the plot represented by the probe is 432,000,000 cm^3. Spatial variability therefore introduces uncertainty in the measurements' interpretation. However, the plots were uniform in terms of soil texture, slope, and crop growth.

In addition, dielectric water potential-based sensors Teros 21 (Meter Group, Inc.) were installed to measure the matric potential over a range of −9 to −2000 kPa (1.96–4.31 pF) with a resolution of 0.1 kPa and an accuracy of 10% between −2000 and −100 kPa and 10% + 2 kPa between −100 and −9 kPa.

At each depth (30–60–90 cm), a Teros 12 sensor and a Teros 21 sensor were placed in parallel for each plot. A total of six sensors were placed in each plot. All 48 probes were connected to eight ZL6 data loggers (Meter Group, Inc.) with two solar panels and connected to ZentraCloud for data retrieval. Measurements are taken every 15 min. In this study, the focus has been placed on the data collected by the sensors at the 30 cm depth only.

2.3 | Meteorological conditions

The 3 years of measurements were very contrasted in terms of meteorological conditions. The year 2021 was a very wet year in Belgium, with a total rainfall of 1039 mm. It was one of the three wettest years since 1991. Precipitation was concentrated in summer, with 410.7 mm of rain, the highest since 1833 (Table 2). The year 2022 was hot and dry, with an average temperature of 12.2°C and total rainfall of 701 mm. It was one of the five driest years since 1991 and the warmest since 1833. March and July, as well as the summer, were the driest on record since 1991. The year 2023 was an intermediate one, with an average temperature of 12.2°C and total precipitation of 1011.4 mm. It was a relatively wet year, especially in spring and autumn. It was the third warmest and fourth wettest year since 1991. June and September 2023 were the hottest months on record since 1833.

2.4 | Drying events

Figure 3 shows the daily rainfall, water content, and matric potential measured continuously for the eight plots at a depth of 30 cm. To compare the temporal evolution of the

TABLE 2 Meteorological conditions for the 3 years of monitoring (2021–2023) and the average between 1991 and 2020 for the four seasons.

Meteorological data	Average (1991–2020)				2021				2022				2023			
	Win	Spr	Sum	Aut	Win	Spr	Sum	Aut	Win	Spr	Sum	Aut	Win	Spr	Sum	Aut
Average T° (°C)	4.1	10.5	17.9	11.2	4.7	8.8	17.8	11.5	5.5	11.3	19.6	12.8	5	10.2	18.9	13.4
Solar radiation (kWh/m^2)	75.5	343.6	442.6	175.8	83	364.6	409.6	184.2	74.8	386.6	483.2	174.9	75.5	319.9	442.6	177
Total rainfall (mm)	228.6	165.6	234.2	209.3	264.1	165.6	410.7	180.6	259	108.8	110.6	210.1	214.9	241.6	279.5	283.7
Days of rainfall	55.2	43.5	42.6	48.5	54	43	50	43	55	23	24	50	54	51	45	52

Note: Values in red, orange, and yellow indicate the highest, one of the three highest and one of the five highest values since 1991. Values in dark blue and light blue represent the lowest values and one of the three lowest values since 1991.

soil water retention between production systems, three drying events per year, 2021–2022–2023, were isolated from the continuous measurements and labelled periods P1–P9.

Several criteria were taken into account when selecting the drying events. Firstly, they had to lead to a reduction in water content and an increase in matric potential. Secondly, preference was given to the most pronounced drying periods. Thirdly, three events per year were chosen to ensure that the whole year was well represented. The three periods per year consecutively correspond to a winter, a spring–summer, and an autumn event, respectively. The duration of the drying phases is 9, 37, and 41 days for 2021, 36, 109, and 45 days for 2022 and 46, 74, and 43 days for 2023 with the most severe drying periods in spring–summer.

To compare the drying periods over time and between plots, the minimum and maximum water contents and matric potential were studied. The slopes of the SWRCs were also analysed. These slopes depend on the drying period and were therefore only compared between plots for the same drying event. To ensure that the same portion of the SWRCs were compared, the slopes were calculated using identical pF values, common to all the plots for each drying period (Table 3). Some slopes could not be calculated due to similar water content values for the pF_{min} and pF_{max} of the drying period. In addition, the slopes of the P9 drying period could not be determined due to the absence of similar SWRCs portions among the eight plots in terms of pF_{min} and pF_{max} values. Slopes were calculated by dividing the difference in pF values by the difference in water content values. The calculations were made using all the digits provided by the probes, that is, three decimals. In the tables, the significant digits have been reduced to two, corresponding to the accuracy of the probes.

2.5 | Soil samplings

2.5.1 | Physico-chemical analysis

For plots T1 (rotations starting in year 1), soil physico-chemical properties were analysed at depths of 30, 60, and 90 cm in June 2021. They were also determined for all the plots at the end of September 2022. Soil particle size distribution was determined using the pipette method (NF X31-107), organic carbon content by dry combustion (NF EN 15936) and pH using a glass electrode (NF ISO 10390).

2.5.2 | Soil bulk density and porosity

In November 2020 and September 2021, soil bulk density was determined for plots T1 using undisturbed soil

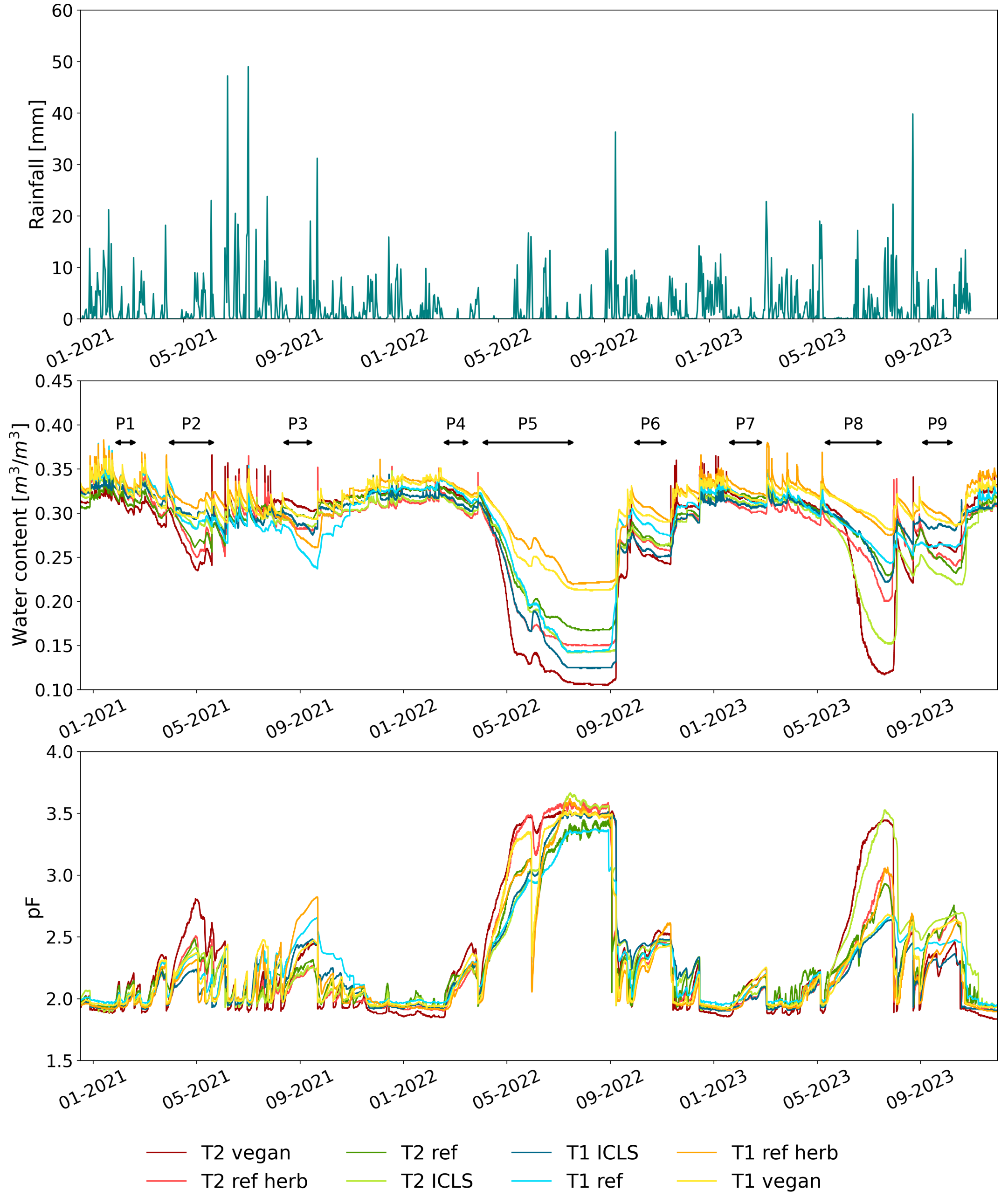

FIGURE 3 Daily rainfall, soil water content and matric potential from January 2021 to December 2023 for the eight plots at a depth of 30 cm. Drying events are indicated by the periods P1–P9.

columns of 8.4 cm diameter and 30 cm length. Undisturbed samples were then taken several times in 100 cm^3 Kopecky rings with a diameter of 5.1 cm and a height of 5 cm. The rings were inserted using a special auger and hammer. The samples were then dried at 105°C for 48 h to determine their bulk density. For all plots, samples were taken at 30 cm in three replicates in March, May, July and September 2022 and in March, July and September 2023. Samples were also taken at 60 and 90 cm in March and September 2022 and in July 2023. Soil porosity was calculated from the bulk density and assuming a soil particle density of 2.65 g/cm^3 and an organic matter particle density of 1.4 g/cm^3.

2.5.3 | Laboratory water retention curve

The SWRC in the unsaturated range was measured in the laboratory using a Ku-pF single-place apparatus (Umwelt-Geräte-Technik GmbH). This device is based on the simplified evaporation method with tension measurements at two depths over time during sample drying,

TABLE 3 Minimum and maximum pF values used to calculate SWRC slopes for each drying period.

Drying event number	Common pF_{min}	Common pF_{max}
P1	1.96	1.97
P2	2.05	2.24
P3	2.17	2.27
P4	1.96	2.24
P5	2.10	3.36
P6	2.24	2.43
P7	1.96	2.10
P8	1.97	2.62
P9	2.47	2.46

combined with continuous weighing. The SWRC is then determined by relating the water content of the sample by weight to the average of the two potentials in kPa measured every 4 min from saturation to a drying limit of −90 kPa.

Undisturbed samples were collected in September 2022 in 250 cm^3 rings, 7.2 cm in diameter and 6.1 cm high, with two holes. Samples were taken using a guide and hammer at a depth of 30 cm in three replicates. Only the T1 plots were sampled because of their different crops in 2021. Samples were first saturated from below for 48 h using filter mesh. The tensiometers were also saturated for 24 h and then calibrated. They were then inserted into the holes in the ring after the soil had been drilled out. SWRCs are measured for tensions ranging from −0.5 to minimum −67.8 kPa (pF 0.70–2.83) with this apparatus.

2.6 | EU-HYDI PTF

Tóth et al. (2015) developed pedotransfer functions applicable for a wide variety of input parameters, relevant to the European continent. Data from the European Hydropedological Data Inventory (EU-HYDI), the largest hydro-pedological database in Europe, was used to train and test these functions (Weynants et al., 2013). The first version of EU-HYDI PTFs present different models and 22 classes. The soil water retention curve $\theta(h)$ can be described by the commonly used van Genuchten equation (van Genuchten, 1980). This equation contains four parameters: the residual water content θ_r, the saturated water content θ_s, the inverse of the air entry value α and the pore size distribution index n. In addition, the parameter m is calculated as $1-(1/n)$. In our study, PTF 21 was chosen because it can be used to determine the van Genuchten parameters from particle size distribution, bulk density and organic matter content. Using a univariate regression tree, it provides the value of θ_r and, using linear regression, the associated values of θ_s, $\log_{10}(\alpha)$, and $\log_{10}(n-1)$. The theoretical EU-HYDI SWRCs for the T1 plots were estimated using particle size distributions, organic carbon content, and bulk density of the samples collected at the end of September 22.

To compare field, laboratory, and theoretical SWRCs, slopes were calculated for a tension between 10 and 67.8 kPa (pF 2–2.83). These common pF values allow the same part of the curve to be compared. These tension values correspond to the overlap of the SWRCs determined by field and laboratory methods.

2.7 | Data treatments

Data from the water content and matric potential sensors for the eight plots from 2021 to 2023 were processed using Python v3.9.13. The figures were plotted with seaborn and matplotlib packages. Analyses of variance (ANOVA) were performed to study differences in bulk density between plots over time. To compare the means, Fisher's Least Significant Difference (LSD) method was used with the null hypothesis of equality of means and a significance level of 0.05. Normality was tested using Shapiro–Wilk and equality of variances using Levene's test. All assumptions were satisfied.

3 | RESULTS

3.1 | Bulk density

The temporal evolution of soil bulk density (ρ_b) for the eight plots studied is shown in Figure 4. Statistical tests were performed on the three spatial replicates of the samples. In September 2021 for T1 plots, ρ_b is significantly higher for T1 ICLS plot with maize (1.64 ± 0.01 g/cm^3) than for T1 vegan with camelina and T1 reference with sugar beets (1.41 ± 0.02 g/cm^3).

In 2022, four samples were taken in March, May, July, and September. In March 2022, after ploughing and sowing winter wheat and winter wheat/peas, the ρ_b of T1 and T2 were close to each other. Then, in May 2022, ρ_b of T1 vegan increased to 1.66 ± 0.05 g/cm^3 and that of T1 ref dropped to 1.44 ± 0.03 g/cm^3. The ρ_b of T2 vegan increased to 1.58 ± 0.06 g/cm^3. It was significantly higher (p value < 0.05) than the other plots, except for T1 vegan. In July 2022, ρ_b were similar for all plots (p value > 0.05) except for the higher T2 vegan and the lower T2 ref herb with 1.46 ± 0.01 g/cm^3. Finally, in September 2022, after

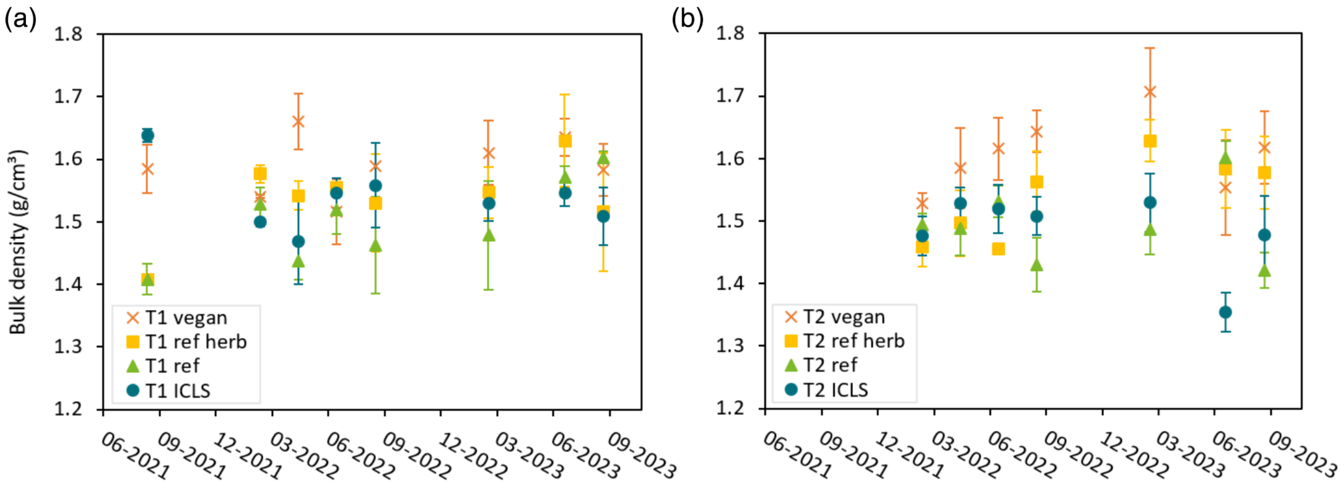

FIGURE 4 Bulk density of the soil in September 2021, March, May, July and September 2022 and in March, July and September 2023 at a depth of 30 cm for plots T1 (a) and T2 (b).

harvesting, the ρ_b values were more differentiated, ranging from 1.46 ± 0.08 to 1.59 ± 0.04 g/cm^3 for T1 and from 1.43 ± 0.03 to 1.64 ± 0.03 for T2. The ρ_b of plots T1 and T2 reference were the lowest, while those of T1 and T2 vegan are the highest.

In 2023, the three samplings were carried out in March, July, and September. In March 2023, after ploughing, T1 ρ_b remained similar for all rotations while T2 ρ_b increased. The ρ_b of T2 vegan increased to 1.71 ± 0.07 g/cm^3 and was higher (p value < 0.05) than the others. Diversified crops were sown in July 2023. In general, ρ_b were similar (p value > 0.05), except for T2 ICLS planted with permanent grassland, which dropped to 1.35 ± 0.03 g/cm^3. Finally, at the end of September 2023, when crops were well developed, T1 ρ_b were generally similar (p value > 0.05), whereas T2 ρ_b were more variable. The ρ_b of T2 ref with maize decreased to 1.42 ± 0.03 g/cm^3. T2 ref and T2 ICLS were lower (p value = 0.05) than the other plots.

Changes in bulk density are generally used to monitor the dynamics of soil structure. These results already show temporal variations in soil structure over time and between plots in response to agricultural practices. However, no clear trend was observed for the growing seasons. These results, based on three soil sampling repetitions, may also depend on spatial variability and capture random behaviour.

3.2 | Temporal evolution of in-situ soil water retention curves

Tables 4 and 5 show the start and end dates of the nine selected drying events, their initial and final SWRC values (θ_{max}, θ_{min}, pF$_{min}$, and pF$_{max}$) and their slope for plots T1 and T2, respectively. For each drying period, to ensure that the same portion of the SWRCs were compared, the slopes between identical pF values, common to all plots were calculated (Table 3). Figure 5 shows SWRCs obtained for the nine drying events, for all plots.

A first observation is that the shape and the position of SWRCs vary between years, within a growing season and between plots. The years are different in terms of SWRC variability. The year 2021 shows the lowest variability in water retention capacity, but the highest variability in slope. In contrast, the year 2023 shows the greatest variability in water retention capacity, demonstrating the impact of production systems and the importance of studies over several years.

Greater variability in SWRCs was observed between plots than over time. This suggests that agricultural practices and differentiated cropping have a greater influence on soil structure than crop development, WDs, and meteorological conditions. The largest differences were found between T1 and T2 plots and between T1 plots. T2 plots are generally more similar, especially in 2021 and 2022. The most different SWRCs are T1 ref with sugar beet and T1 vegan with camelina as well as T1 ref and T1 ICLS with maize in 2021. For 2022, the main differences are observed between T1 ICLS and T1 vegan, respectively with winter wheat and faba bean, and between T1 ref and ref herb without or with herbicide.

Over time, within a growing season, greater variability in SWRCs was observed between wet-drying cycles (WDs), than between years. Thus, root development and WDs seem to have a greater effect on soil water retention than inter-annual meteorological conditions. Within a growing season, the greatest variation was observed for

TABLE 4 Description of the selected drying events with start and end dates, minimum and maximum soil water content (θ_{max}–θ_{min}), maximum and minimum $\log_{10}$ matric potential (pF) (pF_{min}–pF_{max}), and slopes calculated between identical pF values for each drying period (Table 3) for the four plots of temporality 1 of the contrasting production systems studied.

Years	Event number	Start date	End date	T1 ref					T1 herb					T1 ICLS					T1 vegan				
				θ_{max}	θ_{min}	pF_{min}	pF_{max}	Slope	θ_{max}	θ_{min}	pF_{min}	pF_{max}	Slope	θ_{max}	θ_{min}	pF_{min}	pF_{max}	Slope	θ_{max}	θ_{min}	pF_{min}	pF_{max}	Slope
2021	P1	0702-21	16-02-21	0.37	0.33	1.96	2.05	0.6	0.37	0.33	1.92	1.97	—	0.34	0.32	1.91	2.05	16.0	0.36	0.32	1.94	2.03	4.0
	P2	10-04-21	17-05-21	0.34	0.28	2.01	2.36	15.8	0.37	0.31	1.95	2.32	13.6	0.33	0.29	1.94	2.24	7.6	0.35	0.29	1.96	2.37	9.5
	P3	21-08-21	01-10-21	0.29	0.24	2.17	2.65	16.7	0.30	0.26	2.03	2.81	100.0	0.31	0.28	1.97	2.48	50.0	0.32	0.29	1.97	2.47	25.0
2022	P4	23-02-22	31-03-22	0.34	0.31	1.96	2.29	12.6	0.34	0.32	1.91	2.28	27.7	0.32	0.30	1.92	2.28	18.5	0.35	0.32	1.93	2.35	25.2
	P5	09-04-22	27-07-22	0.32	0.14	2.10	3.36	7.1	0.33	0.22	1.97	3.62	16.6	0.31	0.13	2.04	3.52	7.8	0.33	0.21	1.98	3.52	14.8
	P6	02-10-22	16-11-22	0.31	0.27	2.01	2.45	13.6	0.33	0.29	1.97	2.61	21.1	0.28	0.25	2.24	2.48	11.9	0.33	0.29	1.97	2.43	23.8
2023	P7	20-01-23	07-03-23	0.33	0.31	1.96	2.20	8.6	0.34	0.32	1.91	2.19	22.8	0.32	0.31	1.90	2.10	45.7	0.34	0.31	1.92	2.25	22.8
	P8	11-05-23	24-07-23	0.36	0.25	1.97	2.63	8.4	0.40	0.28	1.95	3.06	20.3	0.31	0.22	1.93	2.62	8.2	0.33	0.28	1.96	2.67	19.1
	P9	01-09-23	14-10-23	0.27	0.26	2.39	2.47	—	0.31	0.28	1.96	2.61	—	0.30	0.28	1.96	2.36	—	0.33	0.29	2.06	2.64	—

TABLE 5 Description of the selected drying events with start and end dates, minimum and maximum soil water content (θ_{max}–θ_{min}), maximum and minimum $\log_{10}$ matric potential (pF) (pF_{min}–pF_{max}) and slopes calculated between identical pF values for each drying period (Table 3) for the four plots of temporality 2 of the contrasting production systems studied.

Years	Event number	Start date	End date	T2 ref					T2 herb					T2 ICLS					T2 vegan				
				θ_{max}	θ_{min}	pF_{min}	pF_{max}	Slope	θ_{max}	θ_{min}	pF_{min}	pF_{max}	Slope	θ_{max}	θ_{min}	pF_{min}	pF_{max}	Slope	θ_{max}	θ_{min}	pF_{min}	pF_{max}	Slope
2021	P1	07-02-21	16-02-21	0.35	0.31	1.93	2.11	16.0	0.36	0.32	1.92	2.00	8.0	0.36	0.33	1.90	2.02	—	0.34	0.31	1.88	2.14	16.0
	P2	10-04-21	17-05-21	0.31	0.26	2.05	2.48	27.1	0.35	0.25	1.96	2.51	10.6	0.32	0.28	1.95	2.42	11.2	0.32	0.24	1.90	2.81	15.8
	P3	21-08-21	01-10-21	0.31	0.29	1.97	2.31	12.5	0.30	0.28	1.99	2.27	16.7	0.30	0.28	1.98	2.27	100.0	0.32	0.30	1.91	2.45	33.3
2022	P4	23-02-22	31-03-22	0.33	0.31	1.93	2.27	17.3	0.33	0.29	1.90	2.24	11.5	0.32	0.30	1.93	2.24	14.6	0.33	0.31	1.85	2.45	30.8
	P5	09-04-22	27-07-22	0.32	0.17	2.07	3.41	8.9	0.31	0.15	1.97	3.60	10.9	0.31	0.14	2.02	3.66	8.6	0.32	0.11	2.03	3.52	7.3
	P6	02-10-22	16-11-22	0.29	0.26	1.94	2.46	10.6	0.29	0.26	1.99	2.48	14.6	0.28	0.26	2.16	2.47	13.6	0.32	0.24	1.93	2.55	10.6
2023	P7	20-01-23	07-03-23	0.33	0.32	1.92	2.18	45.7	0.32	0.30	1.91	2.10	19.6	0.32	0.31	1.92	2.10	19.6	0.35	0.31	1.85	2.25	68.5
	P8	11-05-23	24-07-23	0.32	0.23	1.94	2.93	16.2	0.33	0.20	1.95	3.05	15.1	0.32	0.15	1.93	3.53	11.8	0.33	0.12	1.88	3.44	17.5
	P9	01-09-23	14-10-23	0.28	0.23	2.10	2.76	—	0.30	0.24	1.99	2.67	—	0.25	0.22	2.47	2.69	—	0.29	0.26	1.91	2.46	—

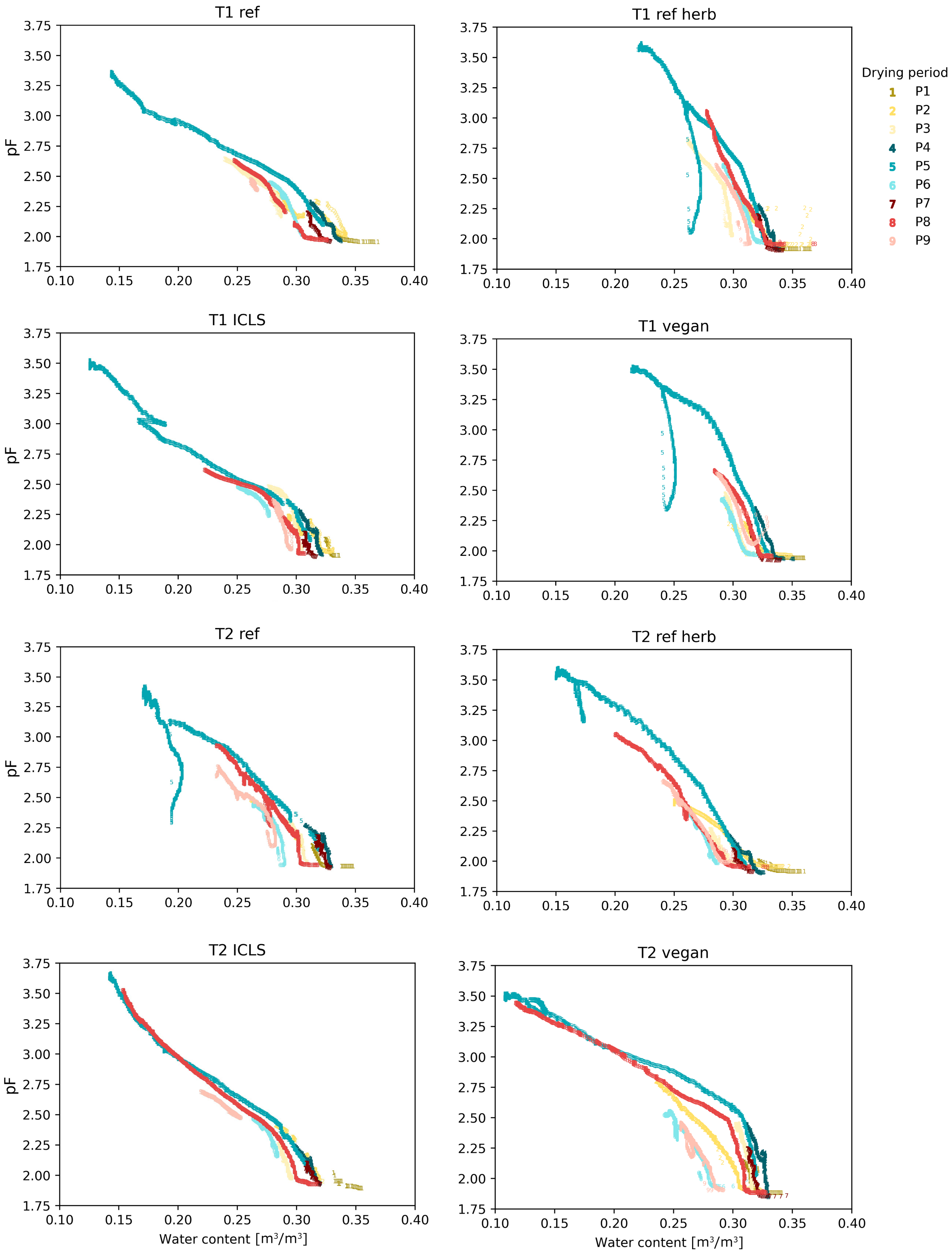

FIGURE 5 SWRCs for drying events P1–P9 from 2021 to 2023 for the eight plots. The drying events are represented by numbers and the years by different colours.

plots T2 vegan in 2022 and T1 ref herb in 2022 and 2023. Between years, the greatest differences were obtained for plots T1 ref and T1 ref herb from 2021 to 2022.

3.2.1 | Temporal evolution over WDs and years

Over time, water retention capacity, and therefore SWRCs shifts, follow the same general trend. During the course of a year, after ploughing, the SWRCs generally shift to the left during the WDs. This means that for the same value of pF, the water content decreases. Thus, the soil water retention capacity decreases between P1 and P3 for 2021, P4 and P6 2022, and P7 and P9 for 2023. The same trend is however not observed for the T1 plots in 2021. In that case, the SWRCs remain similar between P1 and P2 where cover crops are planted. In P2, before and after ploughing and sowing of crops, a discontinuity in SWRCs is observed. Then, between P2 and P3, the same pattern as in the other years is followed, with the SWRCs shifting to the left, indicating a reduction in water retention capacity.

At the beginning of each year, the SWRCs shift to the right, close to the values obtained at the beginning of the previous year. This indicates an increase in water retention capacity during winter and after the harvest. However, as the years go by, the SWRCs shift less to the right. Thus, between 2021 and 2023, decreasing water content close to saturation and retention capacity are noticed.

The steepness of the SWRCs also follows the same general trend, depending on the period and environmental conditions of the year. These differences could be due to the length of the drying periods. Therefore, slopes were only compared between plots for the same drying event. These slopes were calculated between common minimum and maximum pF values for all the plots in order to compare the same portion of the SWRCs.

3.2.2 | Temporal evolution according to agricultural practices and crops

In 2021, water content (θ) generally remained above 0.25 m^3/m^3 for pF between 2 and 2.5. It should be noted that a threshold exists at pF 1.9, which corresponds to the measurement limit of the sensors. Ploughing and rapeseed sowing were carried out before P1 for plots T2. Ploughing and sowing of maize, sugar beet, and camelina took place between P1 and P2 for plots T1. Crops were harvested during or after P3. For T1, the lowest θ_{min} is obtained at P3. Conversely, for T2, the lowest θ_{min} is reached at P2. However, P2 resulted in greater drying for all plots than P3.

During P2, θ_{min} ranged from 0.28 to 0.32 m^3/m^3 for T1 and from 0.24 to 0.28 m^3/m^3 for T2. T2 ref herb retains the least amount of water with a decrease of 0.1 m^3/m^3 to reach a θ_{min} of 0.24 m^3/m^3.

In contrast, at P3, θ_{min} ranged from 0.24 to 0.29 m^3/m^3 for T1 and from 0.28 to 0.30 m^3/m^3 for T2. Decreases in water content were more pronounced for T1 ref and T1 ref herb with sugar beet. The SWRC of T1 ref showed a lower water retention capacity with a flatter slope than T1 ref herb. The SWRC of T1 vegan with camelina shows the greatest water retention capacity.

In general, during 2021, the T2 SWRCs were further to the left and steeper than the T1 SWRCs, indicating a lower water retention capacity and could indicate a more compact soil.

In 2022, the spring–summer drought led to a wider range of the field SWRCs than in 2021. Winter wheat (+peas) was sown after a ploughing before P4 and harvested between P5 and P6.

P4 was the least marked drying period of 2022. θ_{min} range from 0.31 to 0.29 m^3/m^3 for pF between 1.8 and 2.4. The T1 vegan had the highest water retention capacity with a SWRC further to the right. Between P3 at the end of 2021 and P4 at the beginning of 2022, the SWRCs of T1 ref and T1 ref herb with sugar beet in 2021 had the greatest increase in water retention capacity, with a larger shift to the right than for the other plots. In addition, these two plots are steeper despite ploughing. This may indicate greater soil compaction or the influence of non-equilibrium flows and air trapped in the pore network.

P5 is the longest and most severe of the nine selected drying events. The initial θ_{max} and pF_{min} were similar for all plots. However, the final θ_{min} were highly variable between plots. They ranged from 0.13 to 0.22 m^3/m^3 for T1 and from 0.11 to 0.17 m^3/m^3 for T2 for pF between 3.4 and 3.7. For T1, θ_{min} of T1 ref herb was the highest with 0.22 m^3/m^3. Greater water retention capacity was also evident on this plot. Following, T1 vegan had a higher water retention capacity than the other T1 plots cultivated without chemical herbicide. Its θ_{min} was 0.21 m^3/m^3. T1 ref and T1 ICLS followed with lower θ_{min} of 0.14 and 0.12 m^3/m^3. T1 ICLS showed the lowest water retention capacity of all T1 plots as in P4. T2 generally retained less water than T1. T2 vegan showed the greatest drying with a drop of 0.20 m^3/m^3. It also had the lowest water retention capacity of all plots.

At the beginning of P6, the plots had not returned to near-saturation water content. The θ_{max} were therefore more variable than in P4 and P5. As in P5, T2 vegan showed the greatest decrease in water content with θ

falling from 0.32 to 0.24 m^3/m^3. The drying of the other plots was more similar, with decreases in θ between 0.04 and 0.02 m^3/m^3. As in P5, T1 ref herb and T1 vegan have the highest water retention capacities for similar slopes.

In 2023, crops were diversified between plots and SWRCs had varied shapes. Ploughing was carried out before P7 and sowing took place between P7 and P8. Crops were harvested after P9. P7 showed the lowest water loss of 2023 with drying between 0.01 and 0.04 m^3/m^3. The θ_{min} were between 0.31 and 0.32 m^3/m^3 for T1 and 0.30 and 0.32 m^3/m^3 for T2 for pF between 1.9 and 2.2. The retention curves were similar for all the plots.

P8 is the most significant drying event in 2023. Plots T1 ref and T1 ref herb with potato had the highest soil water retention capacity. Their θ_{min} were 0.25 and 0.28 m^3/m^3 respectively. However, T1 ref herb had a SWRC more than twice as steep as T1 ref for the same crop, indicating finer porosity. T1 vegan with faba bean followed and had the lowest decrease in θ (0.05 m^3/m^3). T1 ICLS, also with faba beans, had the lowest retention capacity of T1 plots in 2022. However, it had one of the lowest water drying (0.09 m^3/m^3) of the plots and reached a θ_{min} of 0.22. In general, T2 plots had lower θ_{min} and water retention capacities than T1. In addition, their SWRCs were more similar to each other. The T2 vegan with peas showed the greatest decrease in θ as in 2022 (0.21 m^3/m^3) to reach a θ_{min} of 0.12 m^3/m^3. The T2 ICLS, where the grassland is established, was close with a decrease of 0.17 m^3/m^3 for a θ_{min} of 0.15 m^3/m^3.

At P9, the plots showed the lowest water retention capacities for the 3 years. The θ_{max} were lower than for P7 or P8. T1 ref herb and T1 vegan had the highest water retention capacities, as in 2022 and early 2023. A significant difference between T1 ref herb and T1 ref with potato was observed with higher θ_{max} and θ_{min} with herbicides. T2 had similar water retention capacities, which were still lower than T1 plots. T2 ref and ref herb with maize had the largest dryings (0.05–0.06 m^3/m^3) with θ_{min} of 0.23 and 0.24 m^3/m^3. T2 ICLS with grazed grassland showed the lowest θ_{max} and θ_{min} and the lowest water retention capacity.

3.2.3 | Comparison with laboratory and theoretical SWRCs

Comparisons between EU-HYDI, laboratory and field SWRCs for the year 2022 for the four plots T1 are shown in Figure 6. For T1 ref herb, only two replicates are shown due to inconsistent results for the third replicate. The laboratory SWRCs show variability between replicates, mainly in the wet part of the curves. However, the replicates are similar above pF 2. The laboratory curves reach a limit around pF 3 due to material limitations.

The same trends were found for the four plots. The EU-HYDI SWRCs are generally further to the right, showing higher water retention capacities than the reality in the field. The θ_s are larger for EU-HYDI SWRCs than for the laboratory SWRCs and are generally close to the actual measured porosity. Field SWRCs, on the other hand, are further to the left. The EU-HYDI SWRC seems to be a better fit for the field curves for the plot T1 ref herb, with the most conventional agricultural practices.

The laboratory SWRCs are between the EU-HYDI and field SWRCs. They also show higher water retention capacities than the field reality. These curves were obtained from soil samples taken at the beginning of the third drying period in 2022 (P6). However, the field SWRCs for P6 are the furthest away from the laboratory curves.

The slopes of the EU-HYDI, laboratory, and field P5 SWRCs between pF 2 and 2.83 are shown in Table 6. The P5 was chosen for the comparison because it represents the most significant drying period in 2022. In addition, it allowed the slope to be calculated between the same pF values.

The slopes of the EU-HYDI SWRCs are generally lower than those of the P5 field, mainly for the T1 ref herb and T1 vegan plots. The highest slopes are for T1 ICLS and T1 vegan, due to the higher organic carbon content. The slopes of the laboratory SWRCs are also lower than those of the P5 field SWRCs, but are getting closer. Furthermore, the same trends were found, with steeper curves for T1 ref herb and T1 vegan, as observed for the field curves.

4 | DISCUSSION

4.1 | Temporal evolution of in-situ soil water retention curves

SWRCs varied greatly between years, seasons, and plots. This shows the influence of meteorological conditions, wet-drying cycles (WDs), root development, and agricultural practices on soil structure. This variability has already been reported over time and between different tillage systems (Huang et al., 2021; Pečan et al., 2023; Zhang et al., 2018).

Pečan et al. (2023) showed that root system development and environmental conditions within a season influenced soil structural dynamics and SWRC shape more than tillage system. Our study suggests that agricultural practices and crop differentiation have a greater influence on water retention dynamics than root development and WDs within a season or weather conditions between years. Crop differentiation had the most pronounced effect,

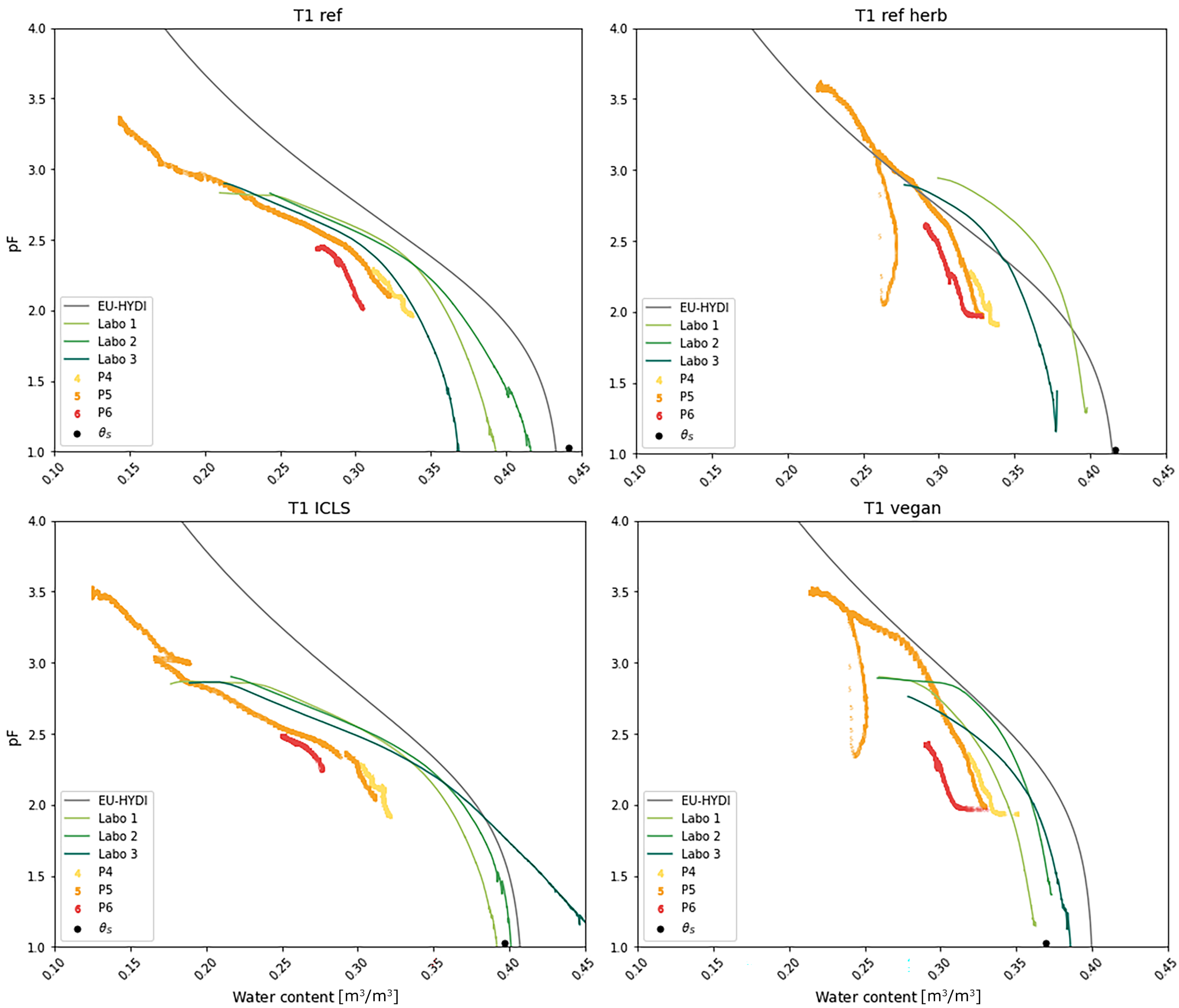

FIGURE 6 Comparison of SWRCs obtained by PTF EU-HYDI, in the laboratory on undisturbed samples and continuously in the field for the year 2022 and the four plots T1. The total porosity measured is shown as a black dot.

TABLE 6 Water contents max and min corresponding to pF of 2 and 2.83 and slope for SWRCs obtained with EU-HYDI PTF, in the laboratory and the field for the P5 drying event.

		T1 ref			T1 ref herb			T1 ICLS			T1 vegan		
SWRC type	Replicate	θ_{max}	θ_{min}	Slope	θ_{max}	θ_{min}	Slope	θ_{max}	θ_{min}	Slope	θ_{max}	θ_{min}	Slope
FPT		0.44	0.29	5.5	0.42	0.29	6.4	0.41	0.3	7.5	0.4	0.32	10.4
Lab	1	0.36	0.21	5.5	0.39	0.33	13.8	0.36	0.24	6.9	0.34	0.29	16.6
	2	0.37	0.24	6.4	—	—	—	0.37	0.24	6.4	0.36	0.31	16.6
	3	0.34	0.23	7.5	0.36	0.3	13.8	0.37	0.22	5.5	0.36	0.28	10.4
Field	P5	0.32	0.22	8.06	0.33	0.29	21.3	0.31	0.2	7.41	0.33	0.3	27.7

followed by weed management. The results also showed a clear effect of soil compaction during harvest and of the establishment of temporary grassland.

It should be noted that the differences between plots may be partly due to spatial variability in the plots studied. The SWRCs analysed were derived from a pair of sensors per plot. The results presented therefore correspond to the volume of influence of the sensors placed in the middle of the plots. Nevertheless, the aim of this study is to investigate the temporal evolution of SWRCs. The sensors were not displaced during the experiment. The differences in the temporal evolutions between plots therefore reflect contrasting changes in soil properties.

The spatio-temporal variability of SWRCs is complex and depends on many physical phenomena. However, not all of these phenomena have been measured and therefore remain hypothetical. The interpretation of the SWRCs variability is based on knowledge of the plots and crops, visual observations, and the most reasonable explanations.

4.1.1 | Temporal evolution over WDs and years

Over time, greater variability in SWRCs has been observed within a growing season than between years. Thus, our study suggests a greater influence of root system development and WDs than of meteorological conditions between years.

In general, water retention capacity decreases over the growing season for relatively stable bulk densities. SWRCs start at progressively lower water contents close to saturation. After each WD, rewetting rates decrease. Similar behaviour has been observed by Herbrich and Gerke (2017). Huang et al. (2021) reported the same trend, but only for non-tillage plots. Typically, a greater variation in water retention capacity was observed after the most intense drying event. These seasonal dynamics may reflect changes in effective wettable porosity and contact angles after each WDs as described by Herbrich and Gerke (2017) and Lourenço et al. (2015). The lower rate of rewetting may also be due to air trapped in the soil pores during drying events (Huang et al., 2021; Zhao et al., 2020). The development of the root system and the increase of biological activity during the growing season may have led to a reduction in the water retention capacity through pore clogging, aggregates breaking up and macropores formation as described by Lu et al. (2020). Large numbers of earthworm galleries were generally observed in all plots during field sampling at 30 cm.

Each year, during the wet and vegetation-free winter period, water retention capacity increases. Ploughing can play a role by aerating the soil to a depth of 25 cm, facilitating water infiltration. Air trapped in the pores can also be released more easily. In fact, our study shows that without winter ploughing, SWRCs are less variable over time, as observed by Huang et al. (2021). Indeed, the SWRCs of plots T1 remained similar between P1 and P2 due to the presence of the cover crops, in contrast to plots T2. The same observation was made for plot T2 ICLS where permanent grassland was established between P6 and P7.

4.1.2 | Temporal evolution according to agricultural practices and crops

Temporal changes in SWRCs are compared with changes in bulk density. The differences observed between systems are interpreted in terms of the factors influencing the hydraulic properties.

Production systems at T1

In 2021, the dynamics of water retention varied between the T1 plots depending on the crop, indicating a short-term effect. T1 vegan with camelina had the highest water retention capacity, probably due to its shallow root system. T1 ICLS and T1 vegan generally had steeper slopes and higher bulk densities than T1 ref, indicating a more compact soil with finer porosity than under sugar beet. The lower water content in plots T1 ref and T1 ref herb may be due to greater water consumption by the beets and higher interception of rainfall by their leaves.

In 2022 and 2023, in the T1 plots without herbicide, T1 vegan had the highest water retention capacity and a steeper slope. It also had a higher bulk density of 1.66 g/cm^3. As a result, the soil is more compact with finer porosity. This plot also produced the highest wheat yield in 2022 with 8.12 t/ha compared to 6.12 t/ha and 6.84 t/ha for plots T1 ref and T1 ICLS. These differences may be due to the chaffing and stubble ploughing of camelina and the use of light agricultural machinery for harvesting. A higher percentage of OM was measured in the soil of this plot in 2022 with 10.4% compared to 2.5% for T1 ref and 5.4% for T1 ICLS. In addition, this plot showed the lowest variability of SWRC over time. The pore system seems to be more stable over time. Thus, following our observations, the vegan production system at T1 should be more resilient in the face of extreme climatic conditions. Our observations are in agreement with Ball et al. (2005) who showed the importance of crop rotation and the addition of OM to the soil to preserve soil structure.

In 2022 and 2023, plot T1 ICLS had the lowest water retention capacity of the T1 plots, despite having a higher OM percentage than T1 ref and ref herb. This may be due to the large and deep root system of maize in 2021. The soil has more interconnected macropores, allowing greater water infiltration. In 2023, despite the presence of faba bean on plots T1 ICLS and T1 vegan, both plots still showed very contrasting water retention behaviour. This contrast demonstrates the influence of the 2021 crop in 2023 and therefore of the rotation in this case. As a result, this production system showed low resilience to drought for T1.

The same crops were planted on plots T1 ref and T1 ref herb. The only difference was the use of synthetic herbicides (ref herb) or shallow hoeing (ref) as weed management strategies. Over the 3 years, T1 ref herb showed greater water retention and less drying out. It had a higher bulk density and a steeper SWRC. As a result, the herbicide-treated plot had finer porosity and a more compact soil at 30 cm. Wheat yields in 2022 were similar (6.12 t/ha), as were OM contents (2.5% and 2.3%). The difference may be due to the higher density of weeds, whose roots took up more water, and the more frequent hoeing in T1 ref, which aerated the soil. Indeed, 5.4 g/m^2 of weeds (dry matter) were measured for T1 ref herb compared to 12.9 g/m^2 for T1 ref.

Between late 2021 and early 2022, T1 ref and T1 ref herb showed a greater increase in retention capacity than the other plots. In addition, their higher bulk densities than at the end of 2021 indicate soil compaction. This compaction may be due to the harvesting of sugar beet with heavy agricultural machinery in November 2021, when the soil was very wet.

In 2023, plots T1 ref and T1 ref herb had higher θ_{max} than the other plots, despite similar bulk densities. The ridges of the potatoes aerated the soil surface, allowing water to infiltrate more easily to a depth of 30 cm. The ridges were also able to retain water for longer, thereby promoting infiltration. The difference may also be due to the lower rainfall interception of the potato crop compared to the faba beans, which contain many weeds and form a denser canopy.

Production systems at temporality 2

Water retention behaviour of T2 plots were more similar than T1 plots and less variable over time.

Over the 3 years, T2 plots showed lower water retention capacity and more severe dryings than T1 plots. During rainfall, water content peaks were more pronounced in T2 than in T1. In 2021, rapeseed was sown on T2 plots from September 2020. In 2021, the rape was well developed and the roots took up more water. In addition, the root development and the macroporosity created by the biological activity have resulted in a more aerated soil with greater water infiltration. The well-developed rapeseed crop with many weeds resulted in a denser canopy. Greater rain interception could partly explain the differences between plots T1 and T2 in 2021. The effect of the extensive root system is still visible 2 years after the end of the crop. The same observation was made for plot T1 ICLS in 2021 and for plots T2 ref and T2 ref herb in 2023 when maize was grown. Deeper, more developed root systems, such as those found in rape and maize crops, can lead to the formation of macropores and greater infiltration of water into the soil. Thus, different crops, and therefore different root systems, can generate different water retention dynamics in the short term.

Permanent grassland was established on plot T2 ICLS in September 2022. In 2023, the pasture grazed by sheep resulted in a significant reduction in water retention capacity and bulk density. The introduction of the grassland could therefore result in soil aeration and increased deep water infiltration capacity. The fact that the soil was left undisturbed resulted in the development of interconnected macropores. These are the result of root growth, canopy density, and biological activity in the soil. Our results contradict those of Jensen et al. (2020). They found an increase in bulk density and no difference in water retention capacity in the short term when a grassland was established. However, they did not plant the same species. In addition, their study focused on the conversion from bare soil to grassland and not from cropland to grassland as in our case.

In 2022 and 2023, the T2 vegan plot had the lowest water retention. In contrast to the other T2 plots, only winter wheat was sown in 2022. The yield was the highest of all plots with 9.36 t/ha. Its OM percentage of 2.84% was comparable to the other plots. In the year 2022, plot T2 vegan had the highest bulk density of all the plots. McDaniel et al. (2014) have shown that rotations with the number of crops and their type lead to the development of macropores due to different plant root systems and biological activity. In our study, the rape-winter wheat-pea rotation produced the lowest water retention of the plots, with the highest porosity and therefore a more aerated soil. Despite the greater water retention capacity and resilience of the vegan production system in T1, the opposite trends were observed for T2.

4.2 | Comparison with laboratory and theoretical SWRCs

The theoretical SWRCs show higher water contents than the other curves. The EU-HYDI database is based on curves obtained in the laboratory using the pressure plate or sandbox method (Tóth et al., 2015). These methods tend to produce SWRCs with higher θ_s than the evaporative methods used in this paper. The steeper slope of the T1 vegan plot could be explained by the higher OC content at 30 cm, due to the shredding and stubble ploughing of the camelina straw. This profile results in greater soil water retention than the other plots.

The EU-HYDI database was chosen because it is more recent and geographically determined for Central Europe

(Tóth et al., 2015). In addition, it takes into account a larger number of factors that strongly influence soil hydrological behaviour. However, the SWRCs obtained with the EU-HYDI PTFs do not provide an acceptable representation of the water retention behaviour for most of the plots. EU-HYDI SWRC fits plot T1 ref herb more closely. Therefore, these PTFs seem to better represent more conventional agricultural practices. As a result, the diversity of management practices for agricultural plots is not sufficiently integrated into the PTFs.

Laboratory SWRCs are between theoretical and field SWRCs, but still show higher water retention capacities than field measurements. Laboratory SWRCs only reflect the water retention of a soil structure condition at the time of sampling.

The slopes of the laboratory SWRCs are close to those of the field and show similar trends between plots. However, they remain lower. In addition, the differences in slope between plots are less pronounced than in the field. Herbrich and Gerke (2017) and Huang et al. (2021) also obtained steeper SWRCs in the field than in the laboratory. The higher soil water retention capacity obtained with laboratory SWRCs can be attributed to the higher water content of undisturbed samples. In fact, saturation of the samples in the laboratory occurs from below. The water flows upwards through the sample, allowing the air in the pores to escape. In the field, however, heavy rainfall usually results in rapid wetting of the soil. This traps air in the soil pores and reduces the water retention capacity. This factor is one of the main causes of the hysteresis phenomenon, which partly explains the differences between the field and laboratory curves (Hannes et al., 2016; Pečan et al., 2023). Huang et al. (2021) also observed that field SWRCs had lower θ for the same pF than laboratory SWRCs. Furthermore, they showed that the effects of different tillage practices were less visible in laboratory SWRCs than in field SWRCs. Therefore, laboratory SWRCs are not optimal for investigating the temporal evolution of water retention properties as a function of meteorological conditions and agricultural practices.

However, the laboratory SWRCs are close to the measured total porosity and allow for the lack of field data below pF 1.96. Due to the lack of field SWRC data, consistency with the laboratory SWRC for the wet part cannot be confirmed. In addition, there is still uncertainty regarding whether full saturation can be achieved in the field.

5 | CONCLUSION

In this study, the impacts of different contrasting production systems and contrasting climatic conditions on the temporal evolution of SWRCs were analysed in the field over 3 years. Field SWRCs were then compared with those obtained using an EU-HYDI PTF and in the laboratory on undisturbed samples.

The results indicate a high degree of variability in SWRCs over time and between production systems. The greatest variability was found between plots, then within a season, and finally between years. This study has therefore shown that agricultural practices and different crops can have a greater influence on soil water retention dynamics than the sole root development and WDs within a season or meteorological conditions between years.

Over a season, water retention decreases with wet-drying cycles (WDs) and root development. This can be due to the decrease in effective wettable porosity as a result of air trapped in soil pores and the development of macropores resulting from the root system and biological activity. After each winter, the water retention capacity increases again as a result of ploughing to 25 cm and high soil moisture. Over the years, however, a decrease in retention capacity has been observed.

Our research shows that agricultural production systems have an influence on soil water retention behaviour. The results suggest that variations in the soil water retention behaviour can be induced by crop differentiation, weed control, crop residue management, compaction during harvest, or the introduction of temporary grassland. Different soil drying dynamics were observed and some agricultural practices were identified as influencing the soil water retention behaviour for at least 2 years. This study therefore shows that agricultural practices and crops can be a lever for contributing to greater food resilience against future climatic conditions. This work has shown that crops and crop rotations can affect soil water retention.

The SWRCs obtained from the EU-HYDI PTFs are not a good representation of the field SWRCs, particularly for non-conventional agricultural practices. As a result, PTFs need to integrate a wider variety of management practices for agricultural plots. The laboratory SWRCs are closer to the field curves with similar trends. However, the differences in SWRCs between different modalities may be less visible. In the short term, these curves are therefore not optimal for investigating the temporal evolution of water retention properties as a function of meteorological conditions and agricultural practices.

Therefore, in order to assess the relevance of production systems for tomorrow's needs, studies should focus on the impact of multi-crop production systems on the dynamics of soil water retention. In addition, continuous measurements of SWRCs in the field should be prioritised. Finally, the variability of soil hydraulic properties in the short, medium, and long term must be taken into account in the models in order to generate more relevant management decisions.

AUTHOR CONTRIBUTIONS

Clémence Pirlot: Conceptualization; methodology; software; validation; formal analysis; investigation; data curation; writing – original draft; writing – review and editing; visualization. **Anne-Catherine Renard:** Software; validation; formal analysis; investigation; data curation; writing – review and editing; visualization; methodology. **Caroline De Clerck:** Methodology; validation; resources; writing – review and editing; supervision. **Aurore Degré:** Conceptualization; methodology; validation; writing – review and editing; resources; supervision; project administration; funding acquisition.

ACKNOWLEDGEMENTS

The authors acknowledge the contribution of the Care Agriculture-Is-Life from the Terra teaching and research centre, which designed, implemented, and supervised the contrasting production systems studied.

FUNDING INFORMATION

This study was funded by the Société Publique de Gestion de l'Eau (SPGE) as part of the Agriculture Is Life for Water Quality project of the Terra teaching and research centre at Gembloux Agro-Bio Tech, Uliege.

CONFLICT OF INTEREST STATEMENT

The authors have no competing interests to declare.

DATA AVAILABILITY STATEMENT

The data that support the findings of this study are available on request from the corresponding author. The data are not publicly available due to privacy or ethical restrictions.

ORCID

Clémence Pirlot https://orcid.org/0000-0002-2982-5335

REFERENCES

Ahmed, A., Alam, J. B., Pandey, P., & Hossain, S. (2021). Estimation of unsaturated flow parameters and hysteresis curve from field instrumentation. *MATEC Web of Conferences*, *337*, 8.

Ajayi, A. E., Horn, R., Rostek, J., Uteau, D., & Peth, S. (2019). Evaluation of temporal changes in hydrostructural properties of regenerating permanent grassland soils based on shrinkage properties and μCT analysis. *Soil and Tillage Research*, *185*, 102–112.

Alletto, L., Pot, V., Giuliano, S., Costes, M., Perdrieux, F., & Justes, E. (2015). Temporal variation in soil physical properties improves the water dynamics modeling in a conventionally-tilled soil. *Geoderma*, *243–244*, 18–28.

Alskaf, K., Mooney, S. J., Sparkes, D. L., Wilson, P., & Sjögersten, S. (2021). Short-term impacts of different tillage practices and plant residue retention on soil physical properties and greenhouse gas emissions. *Soil and Tillage Research*, *206*, 1–12.

Bacq-Labreuil, A., Neal, A. L., Crawford, J., Mooney, S. J., Akkari, E., Zhang, X., Clark, I., & Ritz, K. (2021). Significant structural evolution of a long-term fallow soil in response to agricultural management practices requires at least 10 years after conversion. *European Journal of Soil Science*, *72*, 829–841.

Ball, B. C., Bingham, I., Rees, R. M., Watson, C. A., & Litterick, A. (2005). The role of crop rotations in determining soil structure and crop growth conditions. *Canadian Journal of Soil Science*, *85*, 557–577.

Basile, A., Ciollaro, G., & Coppola, A. (2003). Hysteresis in soil water characteristics as a key to interpreting comparisons of laboratory and field measured hydraulic properties. *Water Resources Research*, *39*, 1–12.

Blanco-Canqui, H., & Wortmann, C. S. (2020). Does occasional tillage undo the ecosystem services gained with no-till? A review. *Soil and Tillage Research*, *198*, 104534.

Bordoni, M., Bittelli, M., Valentino, R., Chersich, S., & Meisina, C. (2017). Improving the estimation of complete field soil water characteristic curves through field monitoring data. *Journal of Hydrology*, *552*, 283–305.

Chandrasekhar, P., Kreiselmeier, J., Schwen, A., Weninger, T., Julich, S., Feger, K. H., & Schwärzel, K. (2018). Why we should include soil structural dynamics of agricultural soils in hydrological models. *Water*, *10*, 1–18.

Ciocca, F., Lunati, I., & Parlange, M. B. (2014). Effects of the water retention curve on evaporation from arid soils. *Geophysical Research Letters*, *41*, 3110–3116.

Dashtaki, S. G., Homaee, M., & Khodaverdiloo, H. (2010). Derivation and validation of pedotransfer functions for estimating soil water retention curve using a variety of soil data. *Soil Use and Management*, *26*, 68–74.

Dey, P., Sundriyal, P., & Sahoo, S. K. (2017). Science of lagging behind-hysteresis in soil moisture characteristic curve – A review. *International Journal of Current Microbiology and Applied Sciences*, *6*, 151–156.

Eat Lancet Commission. (2019). *Healthy diets from sustainable food systems: Summary*.

FAO. (2015). *World reference base for soil resources 2014 – International soil classification system for naming soils and creating legends for soil maps*.

Geris, J., Verrot, L., Gao, L., Peng, X., Oyesiku-Blakemore, J., Smith, J. U., Hodson, M. E., McKenzie, B. M., Zhang, G., & Hallett, P. D. (2021). Importance of short-term temporal variability in soil physical properties for soil water modelling under different tillage practices. *Soil and Tillage Research*, *213*, 105132.

Gozubuyuk, Z., Sahin, U., Cemal, M., & Ozturk, I. (2015). The influence of different tillage practices on water content of soil and crop yield in vetch – Winter wheat rotation compared to fallow – Winter wheat rotation in a high altitude and cool climate. *Agricultural Water Management*, *160*, 84–97.

Guillaume, B., Aroui Boukbida, H., Bakker, G., Bieganowski, A., Brostaux, Y., Cornelis, W., Durner, W., Hartmann, C., Iversen, B. V., Javaux, M., Ingwersen, J., Lamorski, K., Lamparter, A., Makó, A., Mingot Soriano, A. M., Messing, I., Nemes, A., Pomes-Bordedebat, A., Van Der Ploeg, M., … Degré, A. (2023). Reproducibility of the wet part of the soil water retention curve: A European interlaboratory comparison. *The Soil*, *9*, 365–379.

Hannes, M., Wollschlager, U., Wohling, T., & Vogel, H.-J. (2016). Revisiting hydraulic hysteresis based on long-term monitoring of hydraulic states in lysimeters. *Water Resources Research*, *52*, 3847–3865.

Hedayati, M., Ahmed, A., Hossain, M. S., Hossain, J., & Sapkota, A. (2020). Transportation geotechnics evaluation and comparison of in-situ soil water characteristics curve with laboratory SWCC curve. *Transportation Geotechnics*, *23*, 100351.

Heitman, J. L., Kool, D., & Carvalho, H. D. R. (2023). Soil management considerations for water resiliency in a changing climate. *Agronomy Journal*, *115*, 2127–2139.

Herbrich, M., & Gerke, H. H. (2017). Scales of water retention dynamics observed in eroded luvisols from an arable postglacial soil landscape. *Vadose Zone Journal*, *16*, 1–17.

Hu, W., Tabley, F., Beare, M., Tregurtha, C., Gillespie, R., Qiu, W., & Gosden, P. (2018). Short-term dynamics of soil physical properties as affected by compaction and tillage in a silt loam soil. *Vadose Zone Journal*, *17*, 1–13.

Huang, X., Wang, H., Zhang, M., Horn, R., & Ren, T. (2021). Soil water retention dynamics in a Mollisol during a maize growing season under contrasting tillage systems. *Soil and Tillage Research*, *209*, 104953.

Iiyama, I. (2016). Differences between field-monitored and laboratory-measured soil moisture characteristics. *Soil Science and Plant Nutrition*, *62*, 416–422.

Jarvis, N., Groh, J., Lewan, E., Meurer, K. H. E., Durka, W., Baessler, C., Pütz, T., Rufullayev, E., & Vereecken, H. (2022). Coupled modelling of hydrological processes and grassland production in two contrasting climates. *Hydrology and Earth System Sciences*, *26*, 2277–2299.

Jensen, J. L., Schjønning, P., Watts, C. W., Christensen, B. T., & Munkholm, L. J. (2020). Short-term changes in soil pore size distribution: Impact of land use. *Soil and Tillage Research*, *199*, 104597.

Jensen, J. L., Watts, C. W., Christensen, B. T., & Munkholm, L. J. (2019). Soil water retention: Uni-modal models of pore-size distribution neglect impacts of soil management. *Soil Physics & Hydrology*, *83*, 18–26.

Jirků, V., Kodešová, R., Nikodem, A., Mühlhanselová, M., & Žigová, A. (2013). Temporal variability of structure and hydraulic properties of topsoil of three soil types. *Geoderma*, *204–205*, 43–58.

Keller, T., Colombi, T., Ruiz, S., Schymanski, S. J., Weisskopf, P., Koestel, J., Sommer, M., Stadelmann, V., Breitenstein, D., Kirchgessner, N., Walter, A., & Or, D. (2021). Soil structure recovery following compaction: Short-term evolution of soil physical properties in a loamy soil. *Soil Science Society of America Journal*, *85*, 1002–1020.

Kool, D., Tong, B., Tian, Z., Heitman, J. L., Sauer, T. J., & Horton, R. (2019). Soil water retention and hydraulic conductivity dynamics following tillage. *Soil and Tillage Research*, *193*, 95–100.

Lourenço, S. D. N., Jones, N., Morley, C., Doerr, S. H., & Bryant, R. (2015). Hysteresis in the soil water retention of a sand–clay mixture with contact angles lower than ninety degrees. *Vadose Zone Journal*, *14*, 1–8.

Lu, J., Zhang, Q., Werner, A. D., Li, Y., Jiang, S., & Tan, Z. (2020). Root-induced changes of soil hydraulic properties – A review. *Journal of Hydrology*, *589*, 1–13.

McDaniel, M. D., Tiemann, L. K., & Grandy, A. S. (2014). Does agricultural crop diversity enhance soil microbial biomass and organic matter dynamics? A meta-analysis. *Ecological Applications*, *24*, 560–570.

Meurer, K., Barron, J., Chenu, C., Coucheney, E., Fielding, M., Hallett, P., Herrmann, A. M., Keller, T., Koestel, J., Larsbo, M., Lewan, E., Or, D., Parsons, D., Parvin, N., Taylor, A., Vereecken, H., & Jarvis, N. (2020). A framework for modelling soil structure dynamics induced by biological activity. *Global Change Biology*, *26*, 5382–5403.

Meurer, K. H. E., Chenu, C., Coucheney, E., Herrmann, A. M., Keller, T., Kätterer, T., Svensson, D. N., & Jarvis, N. (2020). Modelling dynamic interactions between soil structure and the storage and turnover of soil organic matter. *Biogeosciences*, *17*, 5025–5042.

Pečan, U., Pintar, M., & Kastelec, D. (2023). Variability of in situ soil water retention curves under different tillage systems and growing seasons. *Soil and Tillage Research*, *233*, 1–13.

Piñeiro, V., Arias, J., Dürr, J., Elverdin, P., Ibáñez, A. M., Kinengyere, A., Opazo, C. M., Owoo, N., Page, J. R., Prager, S. D., & Torero, M. (2020). A scoping review on incentives for adoption of sustainable agricultural practices and their outcomes. *Nature Sustainability*, *3*, 809–820.

Pires, L. F., Borges, J. A. R., Rosa, J. A., Cooper, M., Heck, R. J., Passoni, S., & Roque, W. L. (2017). Soil structure changes induced by tillage systems. *Soil and Tillage Research*, *165*, 66–79.

Rabot, E., Wiesmeier, M., Schlüter, S., & Vogel, H. J. (2018). Soil structure as an indicator of soil functions: A review. *Geoderma*, *314*, 122–137.

Sandin, M., Koestel, J., Jarvis, N., & Larsbo, M. (2017). Post-tillage evolution of structural pore space and saturated and near-saturated hydraulic conductivity in a clay loam soil. *Soil and Tillage Research*, *165*, 161–168.

Schwärzel, K., Carrick, S., Wahren, A., Feger, K.-H., Bodner, G., & Buchan, G. (2011). Soil hydraulic properties of recently tilled soil under cropping rotation compared with two-year pasture. *Vadose Zone Journal*, *10*, 354–366.

Schwen, A., Bodner, G., Scholl, P., Buchan, G. D., & Loiskandl, W. (2011). Temporal dynamics of soil hydraulic properties and the water-conducting porosity under different tillage. *Soil and Tillage Research*, *113*, 89–98.

Strudley, M. W., Green, T. R., & Ascough, J. C. (2008). Tillage effects on soil hydraulic properties in space and time: State of the science. *Soil and Tillage Research*, *99*, 4–48.

Tian, Z., Chen, J., Cai, C., Gao, W., Ren, T., Heitman, J. L., & Horton, R. (2021). New pedotransfer functions for soil water retention curves that better account for bulk density effects. *Soil and Tillage Research*, *205*, 1–40.

Tifafi, M., Bouzouidja, R., Leguédois, S., Ouvrard, S., & Séré, G. (2017). How lysimetric monitoring of Technosols can contribute to understand the temporal dynamics of the soil porosity. *Geoderma*, *296*, 60–68.

Tóth, B., Weynants, M., Nemes, A., Makó, A., Bilas, G., & Tóth, G. (2015). New generation of hydraulic pedotransfer functions for Europe. *European Journal of Soil Science*, *66*, 226–238.

van Genuchten, M. T. (1980). A closed-form equation for predicting the hydraulic conductivity of unsaturated soils. *Soil Science Society of America Journal*, *44*, 892–898.

Vogel, H. J., Gerke, H. H., Mietrach, R., Zahl, R., & Wöhling, T. (2023). Soil hydraulic conductivity in the state of nonequilibrium. *Vadose Zone Journal*, *22*, 1–12.

Wahren, A., Feger, K. H., Schwärzel, K., & Münch, A. (2009). Land-use effects on flood generation - considering soil hydraulic measurements in modelling. *Advances in Geosciences*, *21*, 99–107.

Weynants, M., Montanarella, L., Tóth, G., Strauss, P., Feichtinger, F., Cornelis, W., Javaux, M., Matula, S., Daroussin, J., Hennings, V., Schindler, U., Bilas, G., Makó, A., Tóth, B., Romano, N., Iovino, M., Morari, F., Kværnø, S., Nemes, A., … Anaya-Romero, M. (2013). *European HYdropedological Data Inventory*.

Whalley, W. R., Ober, E. S., & Jenkins, M. (2013). Measurement of the matric potential of soil water in the rhizosphere. *Journal of Experimental Botany*, *64*, 3951–3963.

Zhang, M., Lu, Y., Heitman, J., Horton, R., & Ren, T. (2017). Temporal changes of soil water retention behavior as affected by wetting and drying following tillage. *Soil Science Society of America Journal*, *81*, 1288–1295.

Zhang, M., Lu, Y., Horton, R., & Ren, T. (2018). Temporal changes of soil water retention behavior as affected by wetting and drying following tillage. *Soil Physics & Hydrology*, *81*, 1288–1295.

Zhao, Y., Wen, T., Shao, L., Chen, R., Sun, X., Huang, L., & Chen, X. (2020). Predicting hysteresis loops of the soil water characteristic curve from initial drying. *Soil Science Society of America Journal*, *84*, 1642–1649.

How to cite this article: Pirlot, C., Renard, A.-C., De Clerck, C., & Degré, A. (2024). How does soil water retention change over time? A three-year field study under several production systems. *European Journal of Soil Science*, *75*(4), e13558. https://doi.org/10.1111/ejss.13558